Supporting Information

A Singlet Thiophosphoryl Nitrene and Its Interconversion with Thiazyl and Thionitroso Isomers

Hongmin Li,[†] Zhuang Wu,[†] Dingqing Li,[†] Xiaoqing Zeng,*[,†] Helmut Beckers,[§] and Joseph S. Francisco*[,‡]

[†]College of Chemistry, Chemical Engineering and Materials Science, Soochow University, 215123 Suzhou, China [§]Freie Universität Berlin, Institut für Chemie und Biochemie, D-14195 Berlin, Germany

[‡]Department of Chemistry, Purdue University, West Lafayette, 47907 Indiana, USA

Corresponding Author: xqzeng@suda.edu.cn; francisc@purdue.edu

Table of Contents:

Experimental details

Difluorothiophosphoryl azide[1] were prepared according to published protocols. 1-^{15}N sodium azide (98 atom % ^{15}N, EURISO-TOP GmbH) was used for the preparation of ^{15}N labelled samples. Their purity was checked by gas-phase IR spectroscopy.

Matrix IR spectra were recorded on a FT-IR spectrometer (IFS 66v/S Bruker) in a reflectance mode using a transfer optic. A KBr beam splitter and MCT detector were used in the mid-IR region (4000–500 cm^{-1}) and a Ge-coated 6-μ Mylar beam splitter with a He(l) cooled Si bolometer in the far-IR region (700–180 cm^{-1}, CsI window). For each spectrum, 200 scans at a resolution of 0.5 cm^{-1} were co-added.

Gaseous azide sample was mixed with argon in a 1 L stainless-steel storage container. No reaction occurred in the container was proved by checking the IR spectrum of the mixture prior to the pyrolysis experiment. Then a small amount of the mixture was passed through a hot quartz furnace (i.d. 1.0 mm, length 30 mm), which was heated (voltage 2.0 V, current 5.7 A) over a length of ca. 10 mm by a tantalum wire (o.d. 0.25 mm, resistance 0.7 Ω), prior to deposition on the cold matrix support (Ar 16 K, Ne 6 K, Rh plated Cu block) in a high vacuum (~10^{-5} Pa). Details of the matrix apparatus have been described elsewhere.[2]

Matrix UV/Vis spectra were measured with a Perkin-Elmer Lambda 900 UV spectrometer in the range of 200 to 700 nm using a data point distance of 0.5 nm and an integration time of 2 seconds. The radiation from the source and back to the spectrometer was directed through 150 cm long optical quartz fibers, equipped with quartz lenses inside the cryostat, and passed twice through the deposit on a cold Rh mirror.

Photolysis experiments were carried out using various light sources such as (i) an ArF excimer laser (193nm, Lambda-Physik), (ii) a high-pressure mercury arc lamp (TQ 150, Heraeus) by conducting the light through water-cooled quartz lenses combined with various Schott cutoff and interference filters, and (iii) 365 nm LED source (3 Watt power, QIOPTIQ, ML3-UV365) .

Quantum chemical calculation methods

DFT (B3LYP,[3] M06-2X[4]) and *ab initio* (MP2,[5] QCISD,[6] CCSD(T)[7]) calculations on the structures, IR frequencies, and energies were performed at the basis sets of 6-311+G(3df)[8] and aug-cc-pVTZ.[9] Local minima were confirmed by harmonic vibrational frequencies. The transition states were characterized by a single imaginary frequency, and the connection of each transition state was checked by intrinsic reaction coordinate (IRC) calculations at the B3LYP/6-311+G(3df) level.[10,11] The EOM-CCSD method[12] was applied for the prediction of UV-vis spectra. The electronic structures were examined by the natural bond orbital (NBO) analysis[13] as implemented in the Gaussian software package. All reaction enthalpies included zero-point and thermal corrections to 298 K. Quantum chemical calculations were carried out using the Gaussian09 software package.[14]

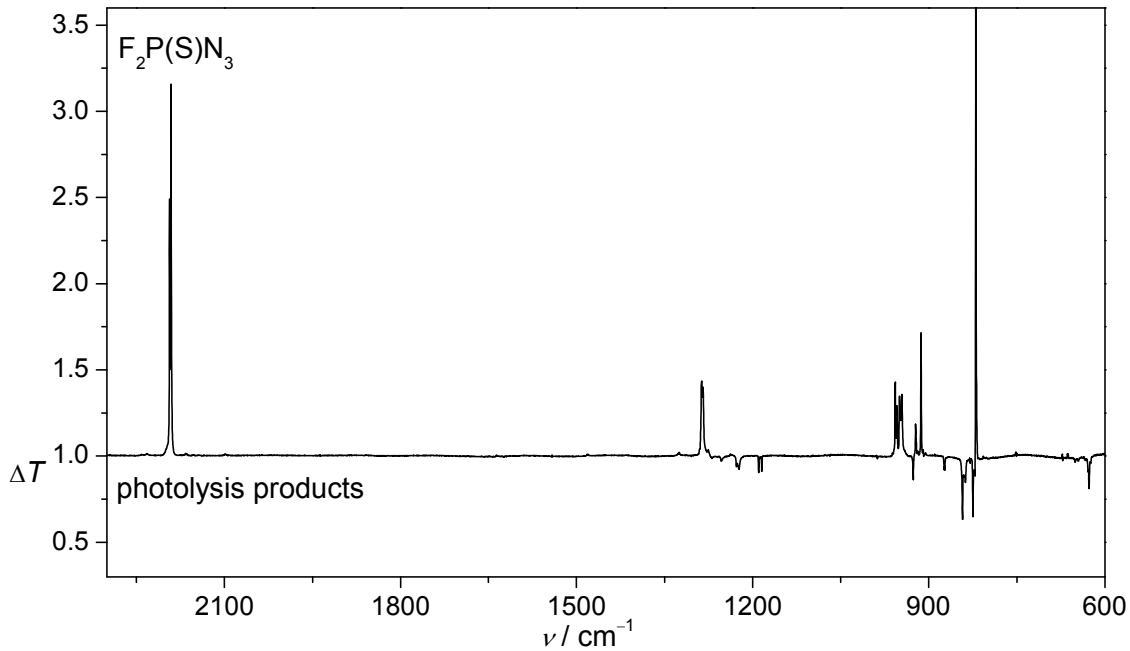

Figure S1. Ar-matrix mid-IR difference spectra (2300–600 cm^{-1}, Transmittance *T*) of the photolysis of $F_2P(S)N_3$ with ArF laser (193 nm, 1.2 mJ, 20 min).

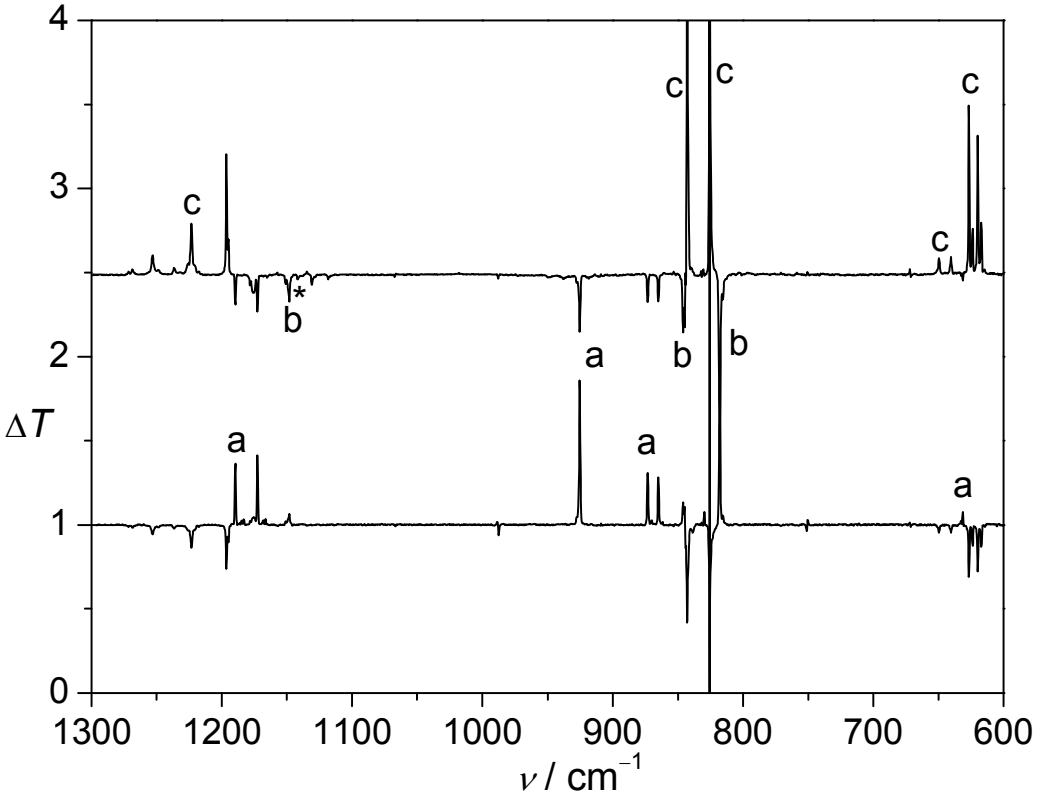

Figure S2. Ar-matrix mid-IR difference spectra (1300–600 cm^{-1}, Transmittance *T*) of: Lower trace: conversion of ^{15}N-labled $F_2P(S)N$ (a) and F_2PSN (b) to F_2PNS (c) under the irradiation of λ = 365 nm (20 min). Upper trace: conversion of ^{15}N-labled F_2PNS (c) to $F_2P(S)N$ (a) and F_2PSN (b) under the irradiation of λ > 495 nm (20 min). A band of an unknown species is labeled by an asterisk.

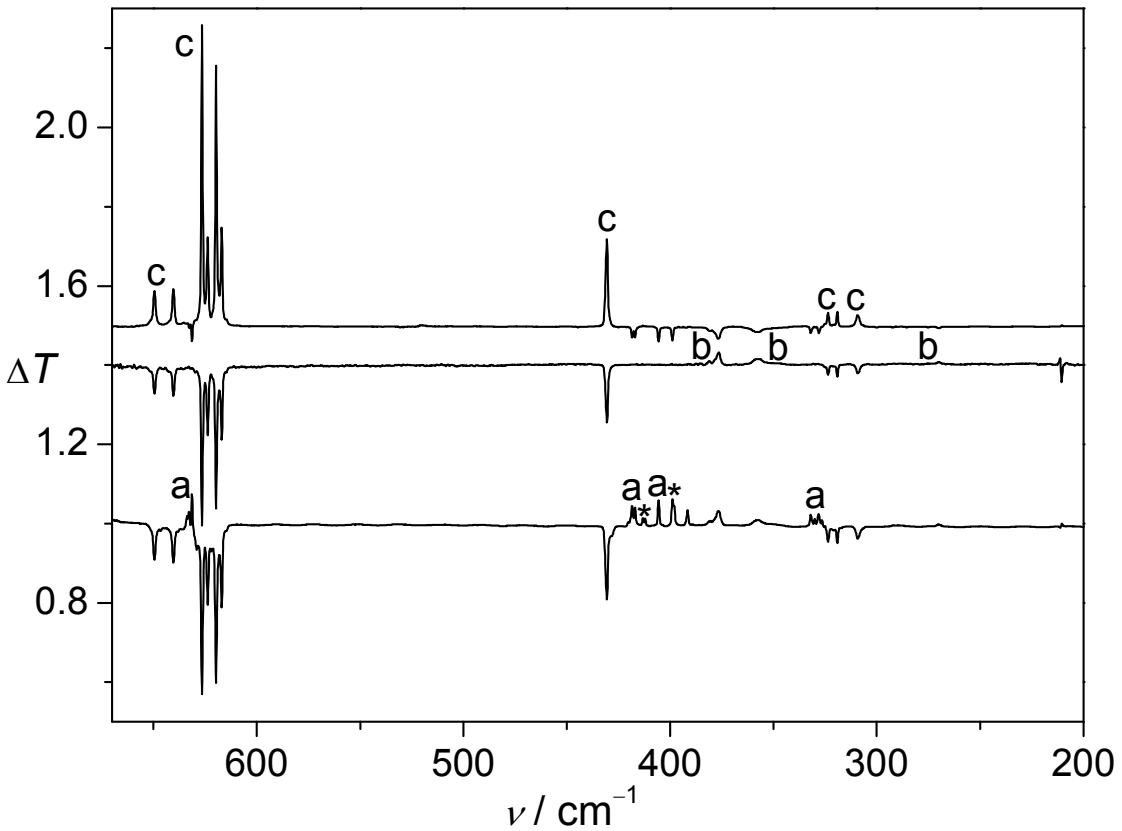

Figure S3. Ar-matrix far-IR difference spectra (670–200 cm^{-1}, Transmittance *T*) of: Lower trace: conversion of ^{15}N-labled $F_2P(S)N$ (a) and F_2PSN (b) to F_2PNS (c) under the irradiation of λ = 365 nm (20 min). Middle trace: conversion of ^{15}N-labled F_2PSN (b) to F_2PNS (c) under the irradiation of λ = 330 nm (16 min). Upper trace: conversion of ^{15}N-labled F_2PNS (c) to $F_2P(S)N$ (a) and F_2PSN (b) under the irradiation of λ > 495 nm (20 min). Bands of unknown species are labeled by asterisks.

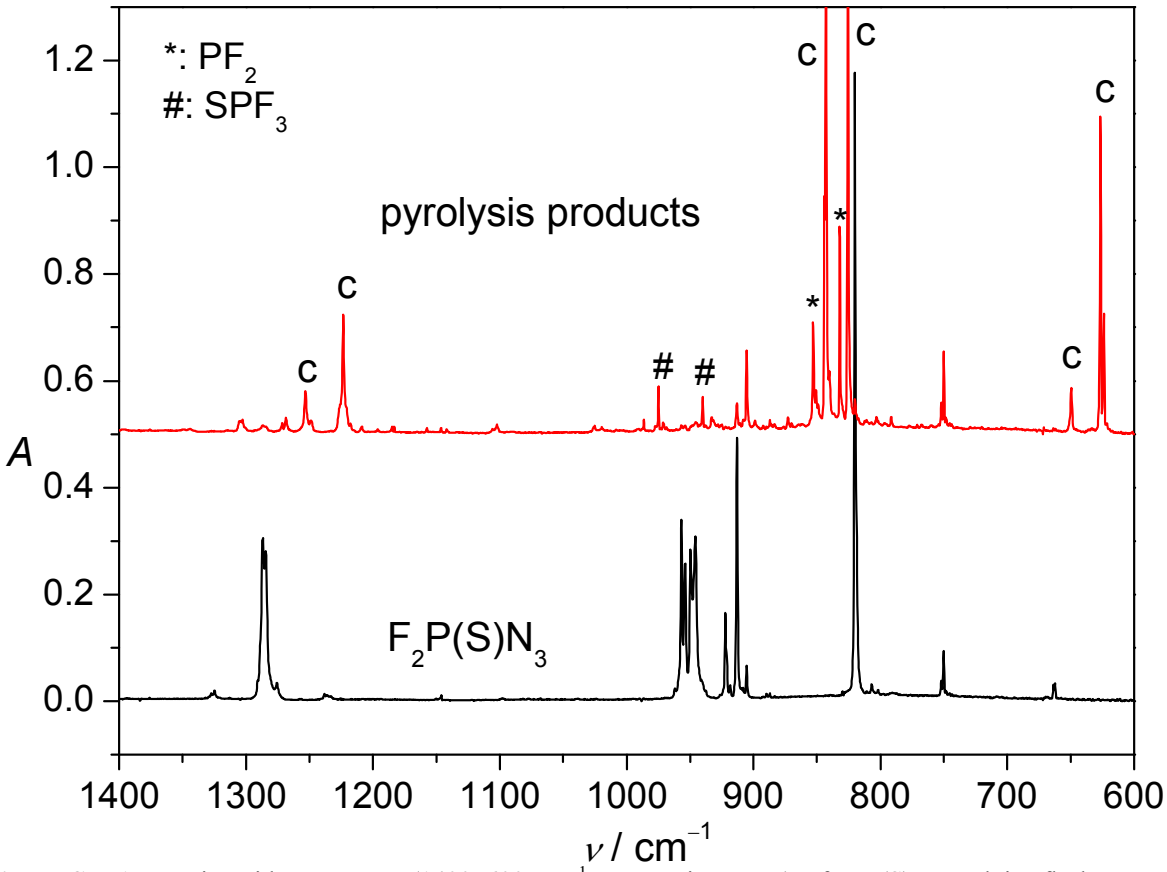

Figure S4. Ar-matrix mid-IR spectra (1400–600 cm^{-1}, Transmittance *T*) of $F_2P(S)N_3$ and its flash vacuum pyrolysis products. The IR bands of F_2PNS (c) are indicated.

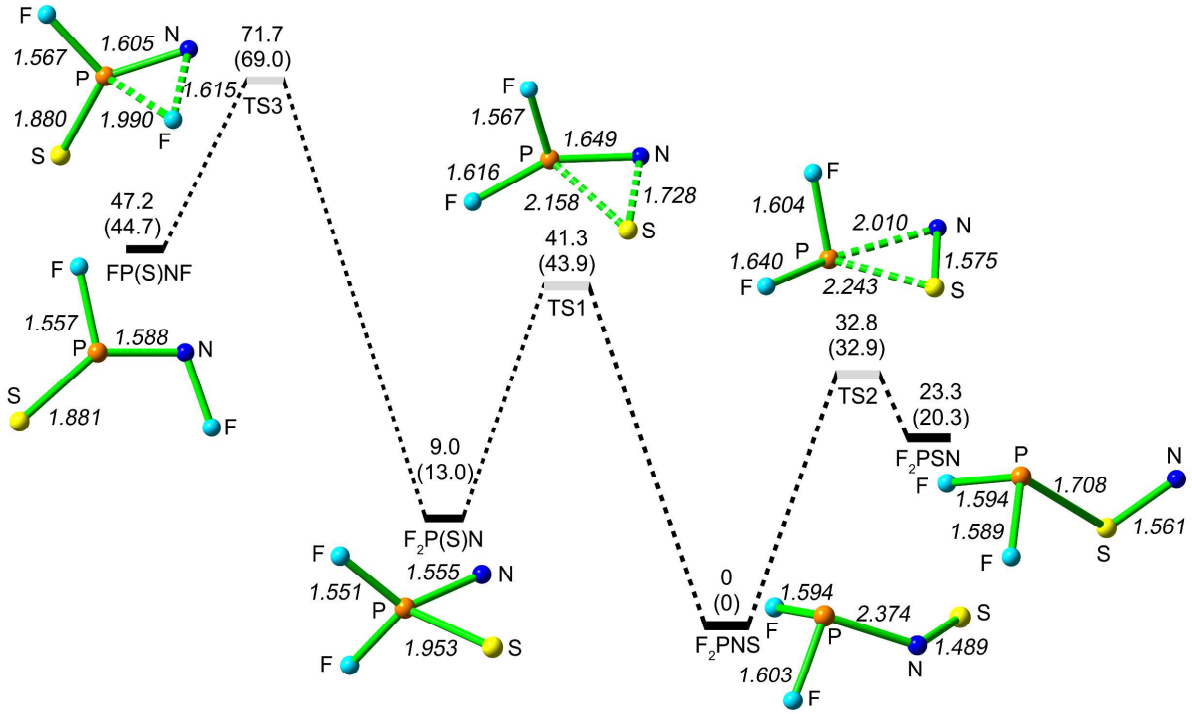

Figure S5. Calculated energy profile (kcal mol^{-1}) for the interconversion of singlet F_2PNS isomers at the CBS-QB3 level. The energies (kcal mol^{-1}, in parentheses) and selected bond lengths (Å, in italics) calculated at the B3LYP/6-311+G(3df) level are also given.

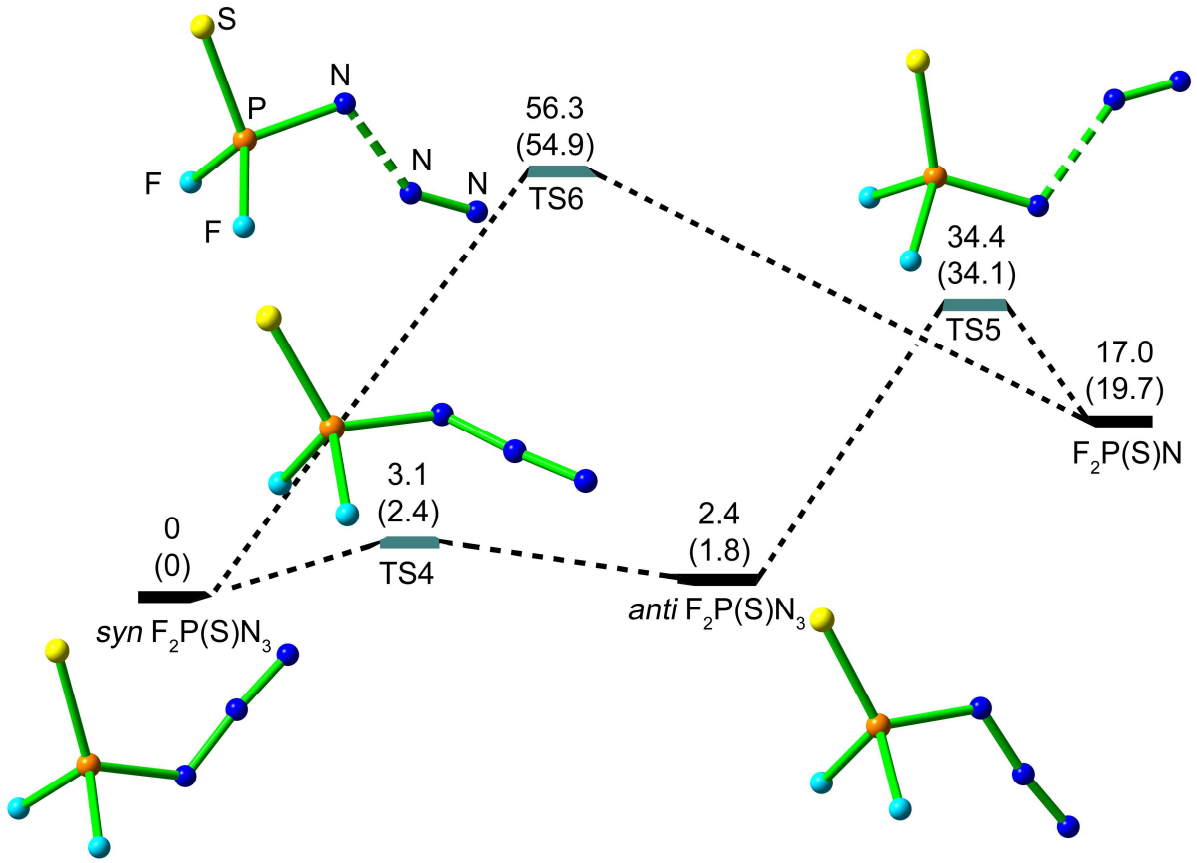

Figure S6. Calculated energy profile (kcal mol^{-1}) for the decomposition of $F_2P(S)N_3$ isomers at the CBS-QB3 and B3LYP/6-311+G(3df) (in parentheses) levels.

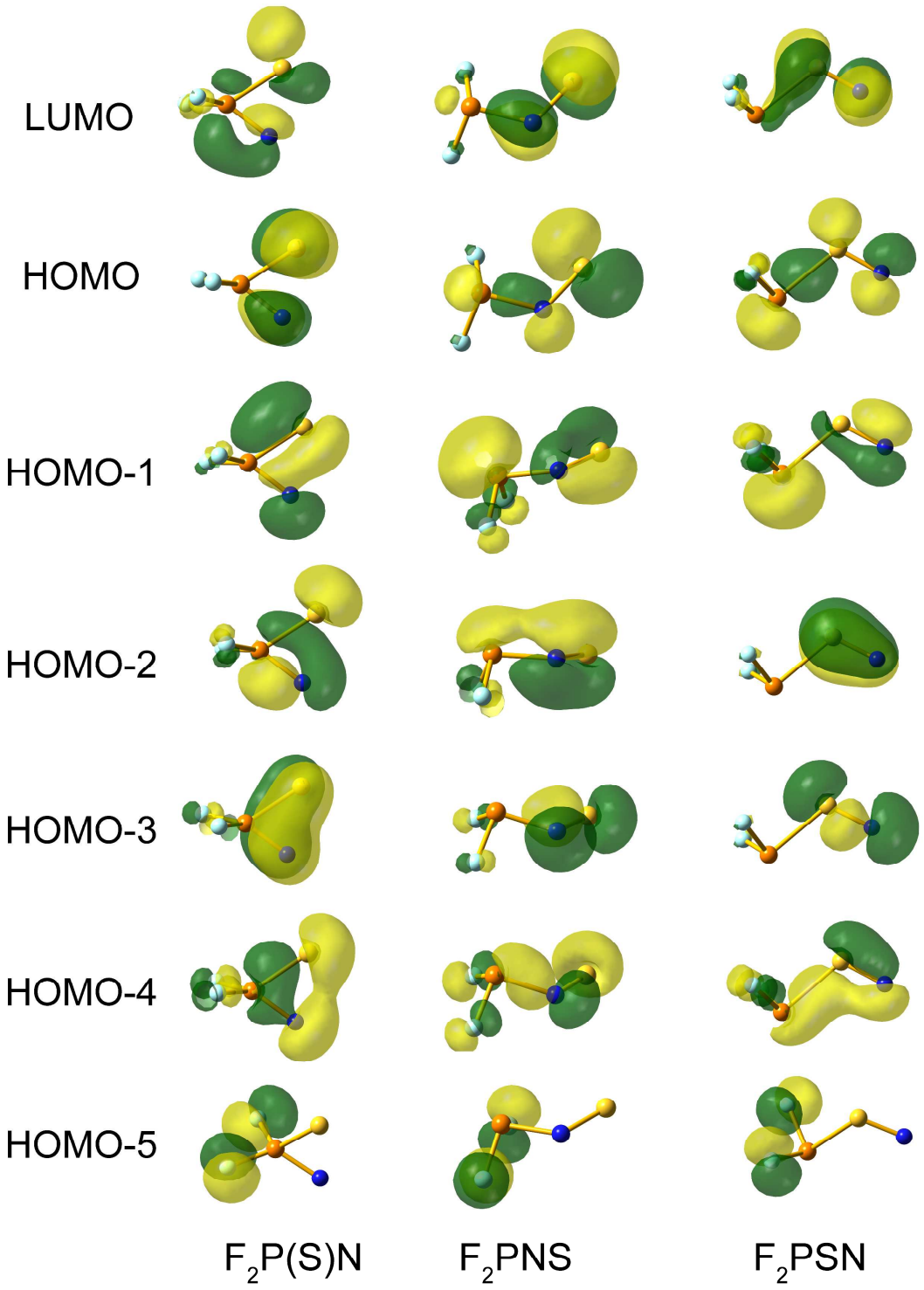

Figure S7. Frontier molecular orbitals (isovalue = 0.05) of singlet $F_2P(S)N$, F_2PNS, and F_2PSN calculated with the MP2/6-311+G(3df) method.

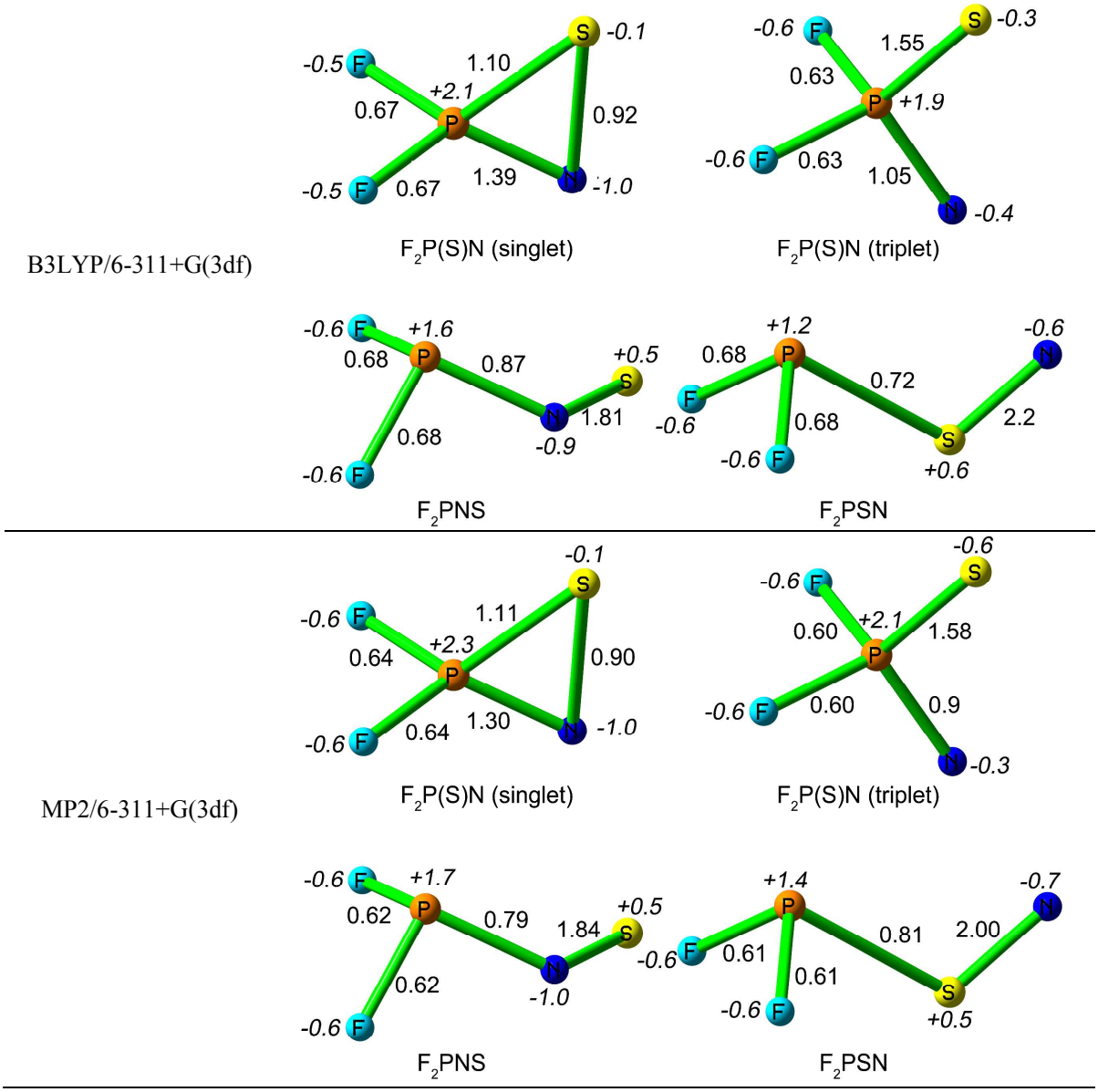

Figure S8. Calculated Wiberg bond index (WBI) and natural population analysis (NPA) charges of F_2PNS isomers with the B3LYP and MP2 methods.

Table S1. Optimized geometries (bond lengths in Å and angles in degrees) for F_2PNS and isomers.

Species	Coordinate	DFT method[a]		Ab initio method[a]		
		B3LYP	M06-2X	MP2	QCISD	CCSD(T)
F_2PNS	r(NS)	1.569	1.553	1.591	1.571	1.586
	r(PN)	1.725	1.722	1.761	1.739	1.747
	r(PF)	1.596	1.583	1.583	1.585	1.587
	r(PF')	1.602	1.588	1.589	1.582	1.591
	θ(SNP)	124.1	122.4	109.6	120.3	119.0
	θ(NPF)	95.6	95.9	96.6	95.7	95.7
	θ(NPF')	103.8	102.2	96.4	101.8	101.8
	τ(SNPF)	135.9	134.0	177.0	138.7	141.1
	τ(SNPF')	36.6	35.4	78.9	40.2	42.6
$F_2P(S)N$ singlet	r(PS)	1.965	1.950	1.958	1.958	1.968
	r(PN)	1.567	1.558	1.562	1.567	1.575
	r(PF)	1.561	1.546	1.548	1.546	1.553
	θ(SPN)	71.9	69.4	69.4	71.7	72.6
	θ(FPN)	123.9	124.1	124.9	123.8	123.9
	τ(FPNS)	115.9	115.2	114.3	115.8	115.9
$F_2P(S)N$ triplet	r(PS)	1.915	1.885	1.877	1.895	1.900
	r(PN)	1.671	1.702	1.713	1.705	1.707
	r(PF)	1.569	1.556	1.557	1.554	1.560
	θ(SPN)	109.6	114.0	115.2	113.4	112.8
	θ(FPN)	107.1	103.0	101.6	103.5	103.9
	τ(FPNS)	127.6	129.0	129.0	128.8	128.7
F_2PSN	r(NS)	1.499	1.498	1.485	1.517	1.516
	r(SP)	2.391	2.288	2.295	2.286	2.334
	r(PF)	1.610	1.593	1.593	1.592	1.597
	r(PF')	1.610	1.597	1.597	1.595	1.600
	θ(NSP)	111.4	105.4	106.9	106.0	106.8
	θ(SPF)	94.8	94.3	92.8	94.8	93.2
	θ(SPF')	94.8	97.5	97.8	97.5	97.2
	τ(FPSN)	131.3	93.6	82.9	90.5	77.0
	τ(F'PSN)	-130.7	-168.5	-178.8	-171.3	-175.3

[a] The basis set of aug-cc-pVTZ was used.

Table S2. Calculated and experimental vibrational frequency (cm^{-1}) for F_2PNS and isomers.

Species	DFT method B3LYP[a]		Ab initio method[b]					mode and symmetry
	ν_i	$\Delta\nu_i(^{14/15}N)$	B3LYP ν_i	M06-2X ν_i	MP2 ν_i	QCISD ν_i	CCSD(T) ν_i	
F_2PNS	1121 (5)	28.0	1105	1173	1023	1132	1068	ν_1, A
	826 (181)	0	828	875	862	873	859	ν_2, A
	801 (137)	0	805	854	844	854	840	ν_3, A
	575 (23)	10.3	568	612	688	629	610	ν_4, A
	420 (25)	3.9	416	436	416	439	425	ν_5, A
	365 (5)	2.2	364	370	326	368	357	ν_6, A
	324 (3)	2.5	319	328	302	324	312	ν_7, A
	138 (2)	0.4	143	161	164	172	164	ν_8, A
	103 (1)	1.4	98	66	66	67	42	ν_9, A
$F_2P(S)N$ singlet	1195 (146)	18.8	1175	1223	1230	1203	1182	ν_1, A'
	900 (153)	0	895	950	934	948	927	ν_7, A"
	855 (140)	7.4	847	888	884	885	868	ν_2, A'
	623 (14)	0.1	617	646	636	643	626	ν_3, A'
	412 (35)	4.9	411	466	493	417	407	ν_4, A'
	397 (14)	3.7	392	408	404	402	393	ν_5, A'
	325 (13)	3.6	319	328	319	329	317	ν_8, A"
	287 (1)	2.2	286	310	307	291	280	ν_6, A'
	112 (<1)	1.2	172	177	170	179	173	ν_9, A"
$F_2P(S)N$ triplet	934 (267)	3.7	924	950	959	958	945	ν_1, A'
	883 (150)	0	879	923	921	932	916	ν_7, A"
	781 (32)	14.6	769	819	853	796	783	ν_2, A'
	640 (2)	1.2	633	666	678	664	657	ν_3, A'
	380 (15)	1.2	376	387	387	391	385	ν_4, A'
	335 (4)	1.0	332	360	369	357	351	ν_5, A'
	309 (14)	2.8	303	314	319	319	311	ν_8, A"
	231 (1)	1.6	229	245	251	248	243	ν_9, A"
	203 (4)	4.3	200	212	217	206	197	ν_6, A'
F_2PSN	1203 (69)	10.5	1184	1206	1283	1117	1141	ν_1, A'
	805 (181)	0	808	857	842	848	835	ν_2, A'
	795 (155)	0	797	847	834	841	828	ν_7, A"
	473 (1)	4.7	467	505	486	495	444	ν_3, A'
	345 (6)	0.5	347	372	364	370	359	ν_4, A'
	193 (2)	2.0	190	221	210	222	214	ν_5, A'
	144 (<1)	0.7	141	201	200	210	190	ν_8, A"
	138 (13)	0.8	137	116	92	116	92	ν_6, A'
	24 (9)	0.2	25	53	37	22	28	ν_9, A"

[a] The basis set of 6-311+G(3df) was used. [b] The basis set of aug-cc-pVTZ was used.

Table S3. Total energy (in Hartree) for F_2PNS and isomers.

Species	DFT Method[a]		Ab initio method[a]		
	B3LYP	M06-2X	MP2	QCISD	CCSD(T)
F_2PNS	-994.154244	-994.008368	-992.894433	-992.780381	-992.825858
$F_2P(S)N$ singlet	-994.129537	-993.987707	-992.880137	-992.757748	-992.805203
$F_2P(S)N$ triplet	-994.139034	-993.981475	-992.858817	-992.758472	-992.796696
F_2PSN	-994.121417	-993.966985	-992.842106	-992.740776	-992.786177

[a] The basis set of aug-cc-pVTZ was used.

Table S4. Relative energies (kcal mol^{-1}) for F_2PNS and isomers.

Species	DFT Method[a]		Ab initio method[a]		
	B3LYP	M06-2X	MP2	QCISD	CCSD(T)
F_2PNS	0.0	0.0	0.0	0.0	0.0
$F_2P(S)N$ singlet	16.2	13.7	10.0	14.9	13.8
$F_2P(S)N$ triplet	15.8	16.9	22.7	13.8	18.5
F_2PSN	19.8	25.2	32.3	24.1	24.9

[a] The basis set of aug-cc-pVTZ was used.

Table S5. Vertical excitation energy (nm) for F_2PNS and isomers.

Species	State	CCSD-EOM aug-cc-PVTZ	*f*
F_2PNS	X^1A	2013	0.0002
		297	0.0297
		260	0.0291
		230	0.0162
$F_2P(S)N$ singlet	X^1A	582	0.0014
		256	0.0173
		255	0.0035
		247	0.0000
$F_2P(S)N$ triplet	X^3A	590	0.0010
		492	0.0085
		390	0.0288
		370	0.000
F_2PSN	X^1A	1069	0.0004
		312	0.0461
		263	0.1351
		250	0.0015

[a]CCSD(T)/aug-cc-PVTZ geometries are used in the calculations.

References:

(1) O'Neill, S. R. ; Shreeve, J. M. *Inorg. Chem.* **1972**, *11*, 1629.

(2) Schnöckel, H. G.; Willner, H. in *Infrared and Raman Spectroscopy, Methods and Applications* (Ed.: B. Schrader), VCH, Weinheim, **1994**.

(3) Becke, A. D. *J. Chem. Phys.* **1993**, *98*, 5648.

(4) Zhao, Y.; Truhlar, D. G. *Theor. Chem. Acc.* **2008**, *120*, 215.

(5) Møller, C.; Plesset, M. S. *Phys. Rev.*, **1934**, *46*, 618.

(6) Pople, J. A.; Head-Gordon, M.; Raghavachari, K. *J. Chem. Phys.* **1987**, *87*, 5968.

(7) (a) Purvis III, G. D.; Bartlett, R. J. *J. Chem. Phys.* **1982**, *76*, 1910. (b) Raghavachari, K.; Trucks, G. W.; Pople, J. A.; Head-Gordon, M. *Chem. Phys. Lett.* **1989**, *157*, 479. (c) Watts, J. D.; Gauss, J.; Bartlett, R. J. *J. Chem. Phys.* **1993**, *98*, 8718.

(8) Frisch, M. J.; Pople, J. A.; Binkley, J. S. *J. Chem. Phys.* **1984**, *80*, 3265.

(9) (a) Dunning, T. H. J. *J. Chem. Phys.* **1989**, *90*, 1007. (b) Kendall, R. A.; Dunning, T. H. J.; Harrison, R. J. *Chem. Phys.* **1992**, 6769.

(10) Gonzalez, C.; Schlegel, H. B. *J. Chem. Phys.* **1989**, *90*, 2154.

(11) Gonzalez, C.; Schlegel, H. B. *J. Phys. Chem.* **1990**, *94*, 5523.

(12) (a) Stanton, J. F.; Bartlett, R. J. *J. Chem. Phys.* **1993**, *98*, 7029. (b) Koch, H.; Kobayashi, R.; Sánchez de Merás, A.; Jørgensen, P. *J. Chem. Phys.* **1994**, *100*, 4393. (c) Caricato, M.*J. Chem. Phys*. **2013**, *139*, 114103.

(13) Reed, A. E.; Curtiss, L. A.; and Weinhold, F. *Chem. Rev.* **1988**, *88*, 899.

(14) Frisch, M. J., Trucks, G. W., Schlegel, H. B., Scuseria, G. E., Robb, M. A., Cheeseman, J. R., Scalmani, G., Barone, V., Mennucci, B., Petersson, G. A., Nakatsuji, H., Caricato, M., Li, X., Hratchian, H. P., Izmaylov, A. F., Bloino, J., Zheng, G., Sonnenberg, J. L., Hada, M., Ehara, M., Toyota, K., Fukuda, R., Hasegawa, J., Ishida, M., Nakajima, T., Honda, Y., Kitao, O., Nakai, H., Vreven, T., Montgomery, Jr., J. A., Peralta, J. E., Ogliaro, F., Bearpark, M., Heyd, J. J., Brothers, E., Kudin, K. N., Staroverov, V. N., Kobayashi, R., Normand, J., Raghavachari, K., Rendell, A., Burant, J. C., Iyengar, S. S., Tomasi, J., Cossi, M., Rega, N., Millam, N. J., Klene, M., Knox, J. E., Cross, J. B., Bakken, V., Adamo, C., Jaramillo, J., Gomperts, R., Stratmann, R. E., Yazyev, O., Austin, A. J., Cammi, R., Pomelli, C., Ochterski, J. W., Martin, R. L., Morokuma, K., Zakrzewski, V. G., Voth, G. A., Salvador, P., Dannenberg, J. J., Dapprich, S., Daniels, A. D., Farkas, Ö., Foresman, J. B., Ortiz, J. V., Cioslowski, J., and Fox, D. J. Gaussian 09, A.1; Gaussian, Inc.: Wallingford CT, 2009

Calculated atomic coordinates (in Angstroms) for F_2PNS isomers and transition states with the B3LYP/6-311+G(3df) methods

$F_2P(S)N$ singlet

N	0.54578100	-0.00014000	1.40541800
P	-0.33810300	-0.00001100	0.12487100
S	1.53164800	0.00003500	-0.43973400
F	-1.29194300	1.16140500	-0.25965000
F	-1.29197700	-1.16134200	-0.25982100

$F_2P(S)N$ triplet

N	0.63464300	1.67619700	-0.00977900
P	0.24503400	0.06575600	-0.00047600
S	-1.64995800	-0.12263400	0.00091700
F	1.01598300	-0.59043200	1.18535600
F	1.01527500	-0.60485400	-1.17858700

F_2PNS

N	0.63490100	-0.73881200	0.10677700
F	-1.75142400	-0.81789000	-0.51078200
F	-0.83969300	1.38074400	-0.24594300
P	-0.85478600	-0.01447800	0.52649400
S	1.98109500	0.02019800	-0.11464500

F_2PSN

F	-0.37806000	1.37959300	1.21084300
F	-0.37806000	1.37959300	-1.21084300
P	0.53860300	0.86502600	0.00000000
S	-0.37806000	-1.32557600	0.00000000
N	0.68214300	-2.37126200	0.00000000

FP(S)NF

F	-0.01094600	1.88239600	0.00000000
N	-1.55248800	-0.01175000	0.00000000
F	-1.72683500	-1.40881500	0.00000000
P	0.00000000	0.32519800	0.00000000
S	1.65671500	-0.56612100	0.00000000

TS1

F	0.00000000	0.00000000	0.00000000
F	0.00000000	0.00000000	2.36205600
P	1.06735500	0.00000000	1.14808700
N	2.44852200	0.51434200	0.40638100
S	2.07411800	1.89581200	1.37561400

TS2

N	0.00000000	0.00000000	0.00000000
F	0.00000000	0.00000000	2.46954600
F	2.28744700	0.00000000	2.54994600
P	1.15233200	-0.60650400	1.53189400
S	1.30980500	0.86041600	-0.15761400

TS3

N	0.00000000	0.00000000	0.00000000
F	0.00000000	0.00000000	2.58730500
F	1.61542600	0.00000000	-0.02269300
P	0.39773000	-0.82714300	1.31712100
S	1.02717500	-2.54488700	1.75028200

syn **$F_2P(S)N_3$**

P	-0.50080100	-0.30217400	0.00000000
N	1.12109000	-0.72907200	0.00000000
N	1.99870600	0.13645600	0.00000000
N	2.86838300	0.84066600	0.00000000
S	-1.01191900	1.51400500	0.00000000
F	-1.01191900	-1.19043500	1.17288300
F	-1.01191900	-1.19043500	-1.17288300

TS4

P	0.00000000	0.00000000	0.00000000
N	0.00000000	0.00000000	1.67369200
N	1.03220200	0.00000000	2.34325500
N	1.90530900	-0.01289600	3.04662100
S	-0.73192900	-1.48263300	-0.89619700
F	1.48046900	0.38896700	-0.34214200
F	-0.67630900	1.37577600	-0.28011900

anti **$F_2P(S)N_3$**

P	0.04240500	0.44950500	0.00000000
N	0.50990600	-1.15527900	0.00000000
N	-0.33072400	-2.06408400	0.00000000
N	-0.99384000	-2.96646900	0.00000000
S	1.43472900	1.70870200	0.00000000
F	-0.99384000	0.51216800	1.17531000
F	-0.99384000	0.51216800	-1.17531000

TS5

P	0.00000000	0.00000000	0.00000000
N	0.00000000	0.00000000	1.60120600

N	1.68994400	0.00000000	2.22827600
N	2.31675200	0.00000000	3.12776600
S	-1.90308400	0.00000000	-0.19336700
F	0.81255200	-1.16491100	-0.64885900
F	0.81255200	1.16491100	-0.64885900

TS6

P	0.00000000	0.00000000	0.00000000
N	0.00000000	0.00000000	1.64105600
N	1.89666700	0.00000000	2.44098900
N	2.45641300	-0.04498200	3.37852600
S	1.41747800	0.92556000	-0.87944200
F	-1.46738700	0.49846600	-0.22425300
F	-0.21350700	-1.45187500	-0.54802300